

NRC Publications Archive Archives des publications du CNRC

Loadbearing capacity of cold formed steel joists subjected to severe heating

Alfawakhiri, F.; Sultan, M. A.

This publication could be one of several versions: author's original, accepted manuscript or the publisher's version. /
La version de cette publication peut être l'une des suivantes : la version prépublication de l'auteur, la version acceptée du manuscrit ou la version de l'éditeur.

Publisher's version / Version de l'éditeur:

Interflam 2001: proceedings of the ninth international conference, vol. 1 (days 1-2, technical papers), pp. 431-442, 2001-10-01

NRC Publications Archive Record / Notice des Archives des publications du CNRC :

<https://nrc-publications.canada.ca/eng/view/object/?id=08f7a689-187f-45d2-85d1-85e9b62d1c75>

<https://publications-cnrc.canada.ca/fra/voir/objet/?id=08f7a689-187f-45d2-85d1-85e9b62d1c75>

Access and use of this website and the material on it are subject to the Terms and Conditions set forth at

<https://nrc-publications.canada.ca/eng/copyright>

READ THESE TERMS AND CONDITIONS CAREFULLY BEFORE USING THIS WEBSITE.

L'accès à ce site Web et l'utilisation de son contenu sont assujettis aux conditions présentées dans le site

<https://publications-cnrc.canada.ca/fra/droits>

LISEZ CES CONDITIONS ATTENTIVEMENT AVANT D'UTILISER CE SITE WEB.

Questions? Contact the NRC Publications Archive team at

PublicationsArchive-ArchivesPublications@nrc-cnrc.gc.ca. If you wish to email the authors directly, please see the first page of the publication for their contact information.

Vous avez des questions? Nous pouvons vous aider. Pour communiquer directement avec un auteur, consultez la première page de la revue dans laquelle son article a été publié afin de trouver ses coordonnées. Si vous n'arrivez pas à les repérer, communiquez avec nous à PublicationsArchive-ArchivesPublications@nrc-cnrc.gc.ca.



NRC - CNRC

Loadbearing capacity of cold formed steel joists subjected to severe heating

Alfawakhiri, F.; Sultan, M.A.

NRCC-45009

A version of this paper is published in / Une version de ce document se trouve dans :
INTERFLAM 2001, 9th International Conference Proceedings, v. 1, pp. 431-442

www.nrc.ca/irc/ircpubs

LOADBEARING CAPACITY OF COLD FORMED STEEL JOISTS SUBJECTED TO SEVERE HEATING

Farid Alfawakhiri * and Mohamed A. Sultan **

*** Canadian Steel Construction Council, Toronto, Canada**

**** National Research Council of Canada, Ottawa, Canada**

ABSTRACT

This paper discusses the behaviour of lightweight steel framed (LSF) unrestrained floors, protected with gypsum board ceilings, in five standard fire resistance tests. Parameters investigated in this test series were joist spacing, number of gypsum board layers in the ceiling membrane, floor cavity insulation and presence of concrete topping in the sub-floor. The fire resistance of LSF floors appears to be essentially governed by the ability of gypsum board to remain in place under fire exposure; other factors are of secondary importance. Retrospective numerical thermal-structural simulations of these tests show good agreement with measured temperature and deformation histories. The development of floor deflections is governed by the thermal bowing of steel joists except for the last one or two minutes in the tests, when “run-away” deformations develop due to the formation of inelastic hinges near mid-span. Evaluation of bending moment resistance of heated joists using current design provisions for cold formed steel structures, adjusted to account for the deterioration of strength and stiffness of steel at elevated temperatures, leads to conservative and fairly accurate predictions of fire resistance.

INTRODUCTION

Lightweight steel framed (LSF) assemblies are increasingly popular in commercial and residential construction in North America because of their non-combustibility, dimensional stability, ease of installation and other advantageous features. In many instances¹, LSF walls and floors must be designed to serve as fire compartment boundaries and provide adequate fire resistance. The current practice of fire resistance rating is based on standard fire endurance tests^{2,3}, which are expensive and time consuming. The ongoing evolution of performance-based codes encourages the development of new, analytical, methods of establishing fire resistance that will provide an alternative to costly testing. Reliable analytical/numerical methods are especially needed when non-standard fire exposures must be considered or the size of the structure precludes standard testing. In this context, three computer programs have been developed recently at the National Research Council of Canada (NRC), in collaboration with the Canadian Steel Construction Council, with the purpose of investigating the thermal and structural behaviour of LSF assemblies under fire attack. Earlier publications^{4,5} describe the application of the TRACE thermal model and STUD structural model in retrospective numerical simulations of six fire resistance tests on loadbearing LSF walls. This paper describes the use of TRACE and JOIST (structural) models to simulate the behavior of unrestrained LSF floor assemblies in five standard fire resistance tests.

FIRE RESISTANCE TESTS

The floor assemblies tested (designated FF-22 through FF-25 and FF-27) were 4800 mm long by 3892 mm wide. Floor framing consisted of galvanized cold formed steel joists spanning across the shorter dimension (effective span 3805 mm). The stability of joists was ensured by channel tracks and web stiffeners at joist ends, blocking at 2-3 locations, flat strap bridging (bottom flange plane) at joist mid-span, and the plywood sub-floor (upper flange plane). All connections were performed using screws – no welding was used. Steel frame fabrication details reflected the common practices used in North America. All steel joists had a C-shaped cross-section, nominally, 203 mm deep by 41.3 mm wide, with 12.7-mm flange stiffening lips and base metal thickness of 1.21 mm (MSG gauge 18). The minimum specified steel yield strength was $F_y = 228$ MPa. In each floor assembly, ten resilient channels, spaced 406 mm o.c., were attached perpendicular to joists to support the gypsum board ceilings. Additional resilient channels were installed in Assembly FF-25 (with one layer of gypsum board) to support gypsum board ends. The resilient channels, 14 mm deep by 58 mm wide, were fabricated from 0.6-mm thick galvanized steel sheets. The channels had a 34-mm wide web, designed to support the gypsum board connections, and one 18-mm

Table 1. Summary of Fire Resistance Tests on Unrestrained LSF Floors.

Specimen number	Joist spacing (mm)	Gypsum board ceiling thickness (mm)	Insulation type (mm)	Sub-floor thickness (mm)	Applied load (kN/m ²)	Fall-off time of gypsum board on exposed side (min)		Structural failure time (min)
						Face layer	Base layer	
FF-22	406	2 × 12.7	-	Plywood (15.9)	2.9	66	73	73
FF-23	406	2 × 12.7	Glass	Plywood (15.9)	2.9	59	63	67
FF-24	610	2 × 12.7	Glass	Plywood (19.0)	1.8	59	65	68
FF-25	406	1 × 12.7	Rock	Plywood (15.9)	2.9	35	N/A	46
FF-27	406	2 × 12.7	Glass	Plywood (15.9+ +Concrete (51.0))	1.9	49	53	61

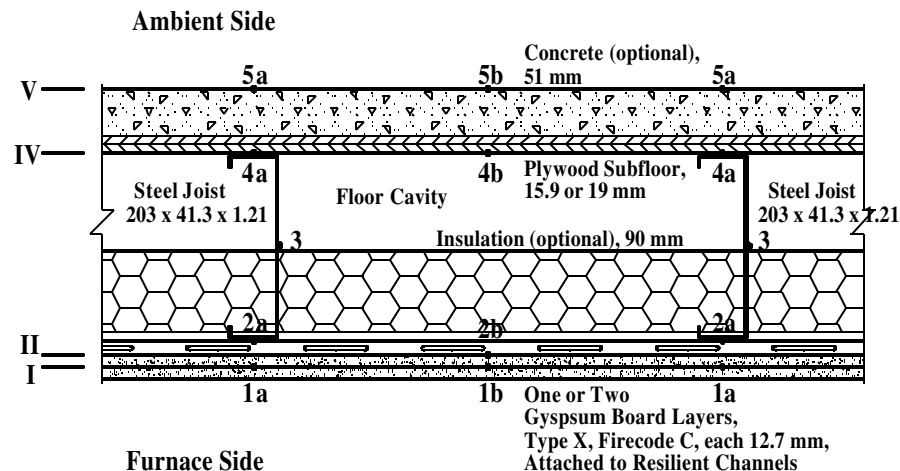


Figure 1. Locations of Temperature Measurements and Simulation Boundaries.



Figure 2. General View of a LSF Floor Assembly after Fire Test.

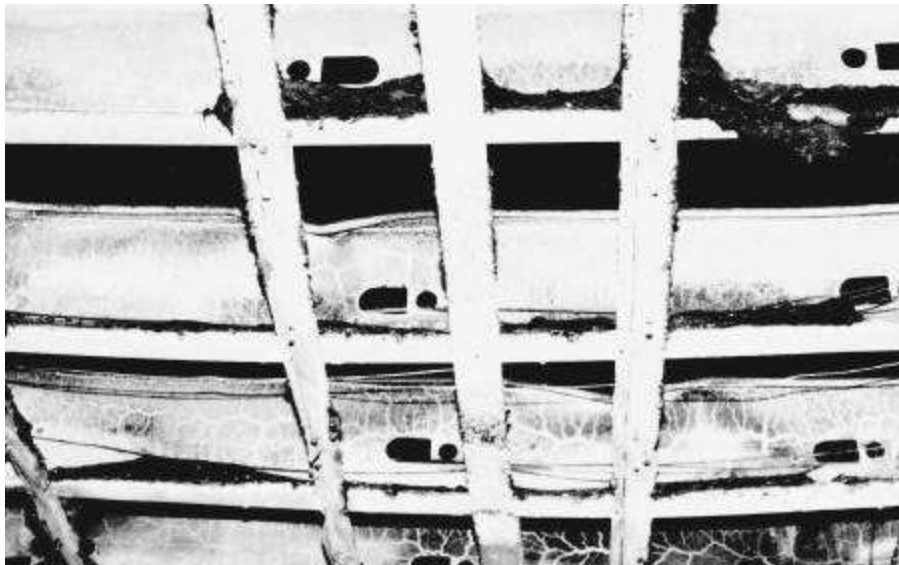


Figure 3. Compressive Failure (Local Buckling) of Top Flanges near Mid-Span.

wide flattened flange lip connected to the bottom flanges of steel joists by 19-mm long self-drilling screws. The cross-sectional details of the floor specimens are illustrated in Figure 1. Complete description of floor construction and test procedures is presented elsewhere⁶.

The gypsum board (nominal thickness 12.7 mm) used in all tests had the “Firecode C Core Type X” designation and met the requirements for Type X gypsum board^{7,8}. It was supplied in 3048×1219-mm sheets. Gypsum board from two different shipments (from the same manufacturer) was used in this test series, and there was a notable difference in the area density of gypsum board used in Test FF-27 (9.55 kg/m²) and that used in Tests FF-22 through FF-25 (10.2 kg/m²). The gypsum board sheets were attached perpendicular to resilient channels by screws 25-41 mm long, spaced 300 mm o.c. along resilient channels.

Table 1 lists the variable parameters of the tests. Two types of insulation were used in this test series: glass fibre batts (10 kg/m^3) and rock fibre batts (33 kg/m^3), both 90 mm thick. The concrete used for the sub-floor in test FF-27 had a density of 2406 kg/m^3 and a compressive strength of 25 MPa (after 28 days). The applied loads in all tests reflect the maximum (100%) load condition, according to CAN/ULC-S101-M89², and steel joist bending strength limit state, according to S136-94⁹.

In addition to standard^{2,3} instrumentation, numerous thermocouples were placed within each floor assembly in order to obtain temperature histories at various locations during fire tests. The generalized locations of these thermocouples are shown in Figure 1 designated by Arabic figures. Figure 4 shows histories of average measured temperatures designated by respective generalized location numbers. Vertical deflections were measured at mid-span and quarter-span locations of three joists in the central part of each floor. The average measured mid-span deflection histories are shown in Figure 5. The temperatures and deflections for Test FF-24 are not shown here due to space limitations, however, these histories are very much similar to those of Test FF-23.

A short summary of test results is provided in Table 1. The listed structural failure times represent the number of completed elapsed minutes for which the floor specimens maintained their ability to sustain the applied load. The structural failure in all tests was manifested through the significant drop in the hydraulic pressure of the loading system and large “run-away” deflections. It was usually accompanied by the penetration of flames and hot gases (integrity failure) through the joints between sub-floor plywood sheets that were opening due to large floor deflections. Figure 2 illustrates a LSF floor assembly after a fire test. Close inspection of steel joists after fire tests indicated that the dominant structural failure mode was the compressive failure (local buckling) of joist top flange near mid-span, as shown in Figure 3. Heat insulation failure was not detected in any of the tests. The maximum temperature rise, measured by thermocouples under standard pads^{2,3} on the unexposed side of floor specimens, reached only 93.1°C (in Test FF-22).

Gypsum board fall-off times, shown in the Table 1, indicate the number of completed elapsed minutes before the fall-off of a layer piece not less than 500 mm in any dimension. These times reflect the beginning of gypsum board layer fall-off. It usually took several minutes for a gypsum board layer to fall-off completely. In all cases, the fall-off occurred due to the deterioration of the mechanical properties of the gypsum board around attachment screws (usually, starting at a corner, or near an end, or an edge of a gypsum board sheet). Close inspection of floor assemblies after fire tests indicated that resilient channels remained properly attached to joists, and board attachment screws remained attached to resilient channels.

The following trends in the behaviour of unrestrained LSF floors, exposed to standard fire, have been established based on experimental observations and measured data:

- Comparison of Tests FF-23 and FF-24 suggests that joist spacing has no effect on the fire resistance of LSF floors. Contrary to generally held belief, wider joist spacing in LSF floors should not be associated with a reduction in their fire resistance (provided that the protective ceiling is not attached directly to the joists).
- One layer of 12.7-mm thick fire resistant gypsum board provides about 15 minutes delay, and 2 layers of 12.7-mm thick fire resistant gypsum board provide about 40 minutes delay, in the temperature rise in the bottom flanges of steel joists (generalized location 2).

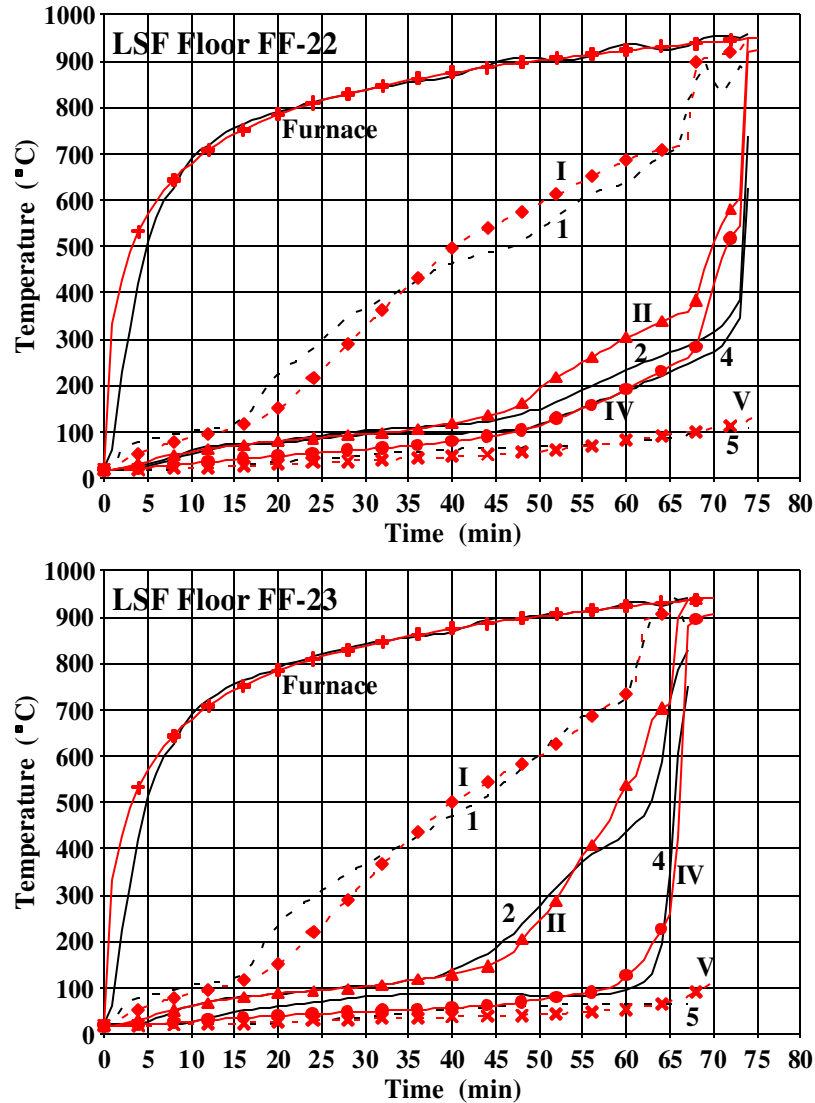


Figure 4. Measured and Simulated Temperature Histories.

- Insulation restricts the passage (and dissipation) of heat through the floor cavity causing an accelerated temperature rise in the bottom flanges (and in the gypsum board ceiling), and a delayed temperature rise in the top flanges of the joists. Therefore, the heating regime in insulated floors features high temperature gradients across the steel joist section, while the heating regime of joists in non-insulated floors is rather close to uniform heating. The development of higher temperature gradients in insulated floors cause larger deflections, due to the associated thermal bowing of joists, compared to non-insulated floors.
- Temperature data from Test FF-25 suggests that steel joists can maintain their loadbearing capacity even when bottom flange temperatures exceed 800°C. The temperature rise in the top flange appears to be more critical.
- The fire resistance of LSF floors is governed by the ability of the gypsum board ceiling to remain in place. This is especially evident in non-insulated floor Test FF-22, where the structural failure occurred immediately after the base gypsum layer began to fall-off and joist top flanges became directly exposed to furnace fire. Glass fibre insulation in tests FF-23 and FF-24 was not able to delay the critical heating of joist top flanges by more than 3-4 minutes,

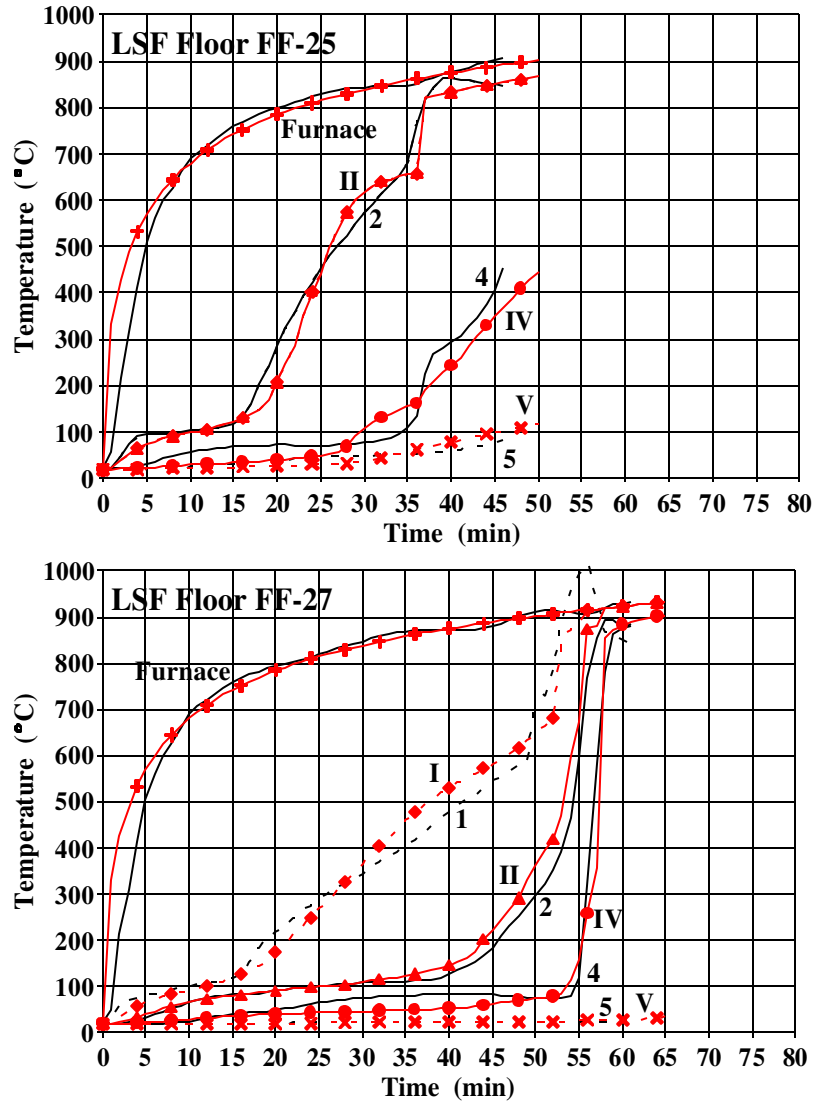


Figure 4 (continued). Measured and Simulated Temperature Histories.

after the fall-off of the gypsum board, because the glass fiber insulation melts when directly exposed to fire. In contrast to that, rock fibre insulation (which does not melt) in Test FF-25 delayed the critical heating of joist top flanges (thus, delaying the structural failure) by 11 minutes after the fall-off of the gypsum board ceiling.

- Comparison of gypsum board fall-off times in Tests FF-22 through FF-24 suggests that accelerated temperature rise in the ceilings of insulated LSF floors reduces the ability of gypsum board to remain in place by 7-10 minutes. As a result, it may be concluded, that glass fibre insulation placed in floor cavity reduces the fire resistance of LSF floors by about 5 minutes. This trend, however, does not apply to rock fibre insulation because of the delaying effect described in the previous paragraph.

HEAT TRANSFER SIMULATIONS

One-dimensional heat transfer numerical simulations were conducted for all tests using the computer program TRACE. Figure 1 shows the locations of simulation boundaries, designated by Roman figures. Simulated temperature histories, at these boundaries, are

Table 2. Apparent Thermal Properties of Type X Firecode C Gypsum Board (bulk density 750 kg/m³).

Apparent thermal properties	Temperature range (°C)											
	<50	50-80	80-100	100-120	120-140	140-160	160-180	180-200	200-300	300-500	500-700	>700
Conductivity [W/(m°C)]	0.27	0.27	0.27	0.15	0.15	0.15	0.15	0.15	0.17	0.17	0.25	0.45
Heat capacity [MJ/(m ³ °C)]	0.49	0.70	1.4	2.8	5.6	9.1	7.0	2.8	2.8	1.4	0.49	0.35

Table 3. Apparent Thermal Properties of Insulation Materials.

Insulation type (bulk density in kg/m ³)	Apparent heat capacity [MJ/(m ³ °C)]	Apparent thermal conductivity [W/(m°C)] in temperature range (°C)						
		<80	80-200	200-300	300-400	400-500	500-700	>700
Rock fibre batts (33 kg/m ³)	0.027	1.0	0.50	0.10	0.10	1.5	2.0	3.0
Glass fibre batts (10 kg/m ³)	0.009	1.0	0.50	0.10	0.10	1.5	2.0	3.0

Table 4. Apparent Thermal Properties of Softwood Plywood (bulk density 450-500 kg/m³).

Apparent thermal properties	Temperature range (°C)						
	<100	100-200	200-250	250-300	300-350	350-500	>500
Conductivity [W/(m°C)]	0.15	0.2	0.2	0.1	0.1	0.1	0.15
Heat capacity [MJ/(m ³ °C)]	0.75	2.4	1.3	1.3	0.4	0.55	0.55

Table 5. Apparent Thermal Properties of Concrete (bulk density 2400 kg/m³).

Apparent thermal properties	Temperature range (°C)						
	<100	100-200	200-400	400-500	500-600	600-800	>800
Conductivity [W/(m°C)]	1.8	1.8	1.55	1.55	1.4	1.4	1.1
Heat capacity [MJ/(m ³ °C)]	1.9	2.5	2.5	3.5	3.5	2.5	2.5

shown in Figure 4 (curves with symbols). The apparent thermal properties of floor materials at elevated temperatures, used in these simulations, are listed in Tables 2-5.

The choice of thermal properties for gypsum board and insulation materials has a major influence on the shape of the simulated temperature curves. Conductivity and heat capacity values, listed in Tables 2 and 3, had already produced good results in previous simulations of six LSF wall tests⁴. Application of these properties in floor test simulations also produced a good match with measured temperature histories. The higher area density of gypsum board sheets in Tests FF-22 through FF-25 was modelled by proportionately increasing the thickness of gypsum board layers from the nominal value of 12.7 mm to 13.5 mm. The choice of thermal properties for plywood and concrete was of little significance, because these materials were located away from the fire exposed side. Values listed in Tables 3 and 4 are based on properties suggested by Lie¹¹. The presence of steel frame was neglected in thermal simulations, because, due to light weight, it plays a minor role in the heat transfer across LSF floors. Sensitivity studies also indicated that temperature histories are not very much affected by the choice of emissivity and convection coefficients.

The fall-off of gypsum board layers is manifested in respective temperature histories by

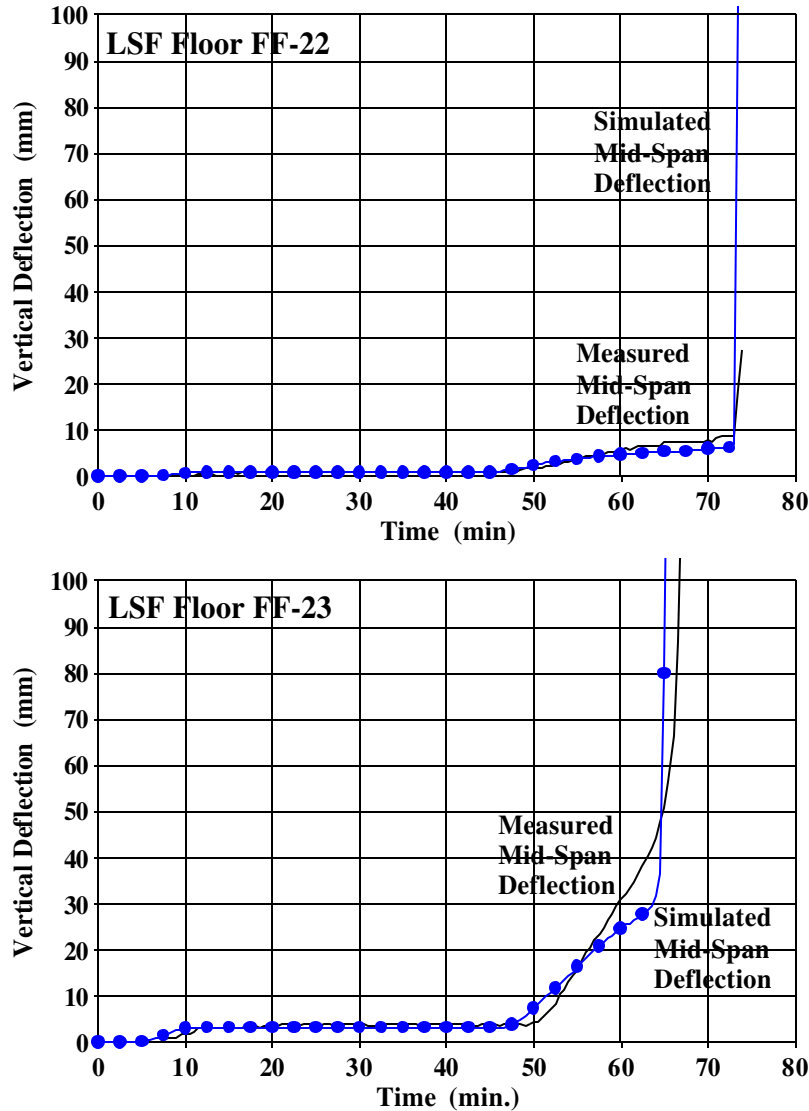


Figure 5. Measured and Simulated Mid-Span Deflection Histories.

sudden shifts in temperature (closely approaching furnace temperature). TRACE models gypsum board fall-off (and melting of glass fibre insulation) by removing the respective layer from the simulation at user-specified time. The fall-off times in Table 1 reflect the beginning of gypsum board layer fall-off based on visual observations. In numerical simulations of Figure 4, these times were slightly adjusted (increased by 1-2 minutes) in order to represent a time when a significant portion of the layer had fallen off.

STRUCTURAL SIMULATIONS

The special purpose computer program JOIST was developed to simulate deflection histories of unrestrained LSF floors exposed to fire and generate predictions of structural failure times. The computational model is based on the following assumptions:

- LSF floor is modelled by a single unrestrained simply supported joist subjected to vertical tributary line load, w , due to applied load and floor self-weight.
- Lateral and torsional failure modes are prevented by adequate lateral restraints.
- Sub-floors do not contribute to bending resistance of LSF floors.

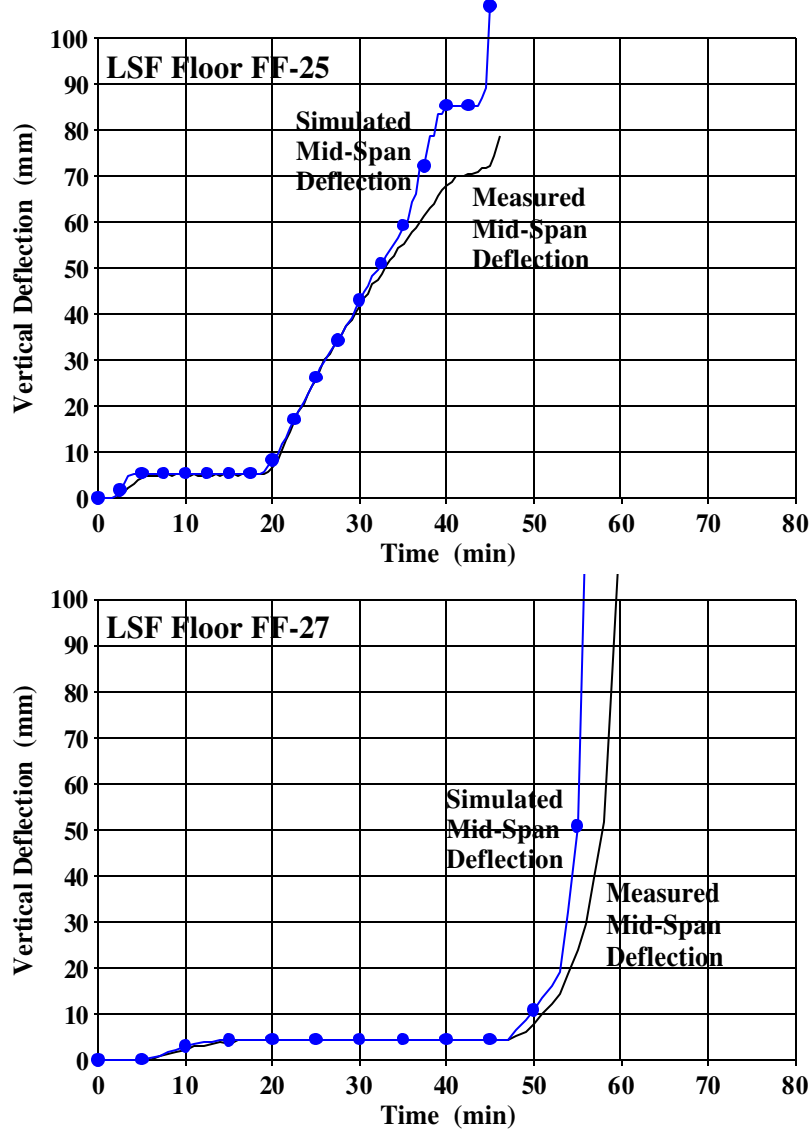


Figure 5 (continued). Measured and Simulated Mid-Span Deflection Histories.

- There is no temperature variation in the horizontal direction along the joist; however, the temperature varies across the joist section from T_H at the hot (bottom) flange to T_C at the cold (top) flange.
- Steel stress-strain relationships at elevated temperatures are linear up to the yield strength.

For the simulations presented in this paper, the following steel properties at elevated temperatures were adopted^{10,11} (extended to 1000°C, as shown in Figure 6):

$$F_{yT} / F_y = (1.0 - 5.3 \cdot 10^{-4} T + 4.0 \cdot 10^{-6} T^2 - 1.9 \cdot 10^{-8} T^3 + 1.7 \cdot 10^{-11} T^4) \quad \text{for } T < 650^\circ\text{C} \quad [1]$$

$$E_T / E = (1.0 - 3.0 \cdot 10^{-4} T + 3.7 \cdot 10^{-7} T^2 - 6.1 \cdot 10^{-9} T^3 + 5.4 \cdot 10^{-12} T^4) \quad \text{for } T < 650^\circ\text{C} \quad [2]$$

$$e_T = (0.2 \cdot 10^{-8} T^2 + 1.2 \cdot 10^{-5} T - 2.408 \cdot 10^{-4}) \quad [3]$$

where

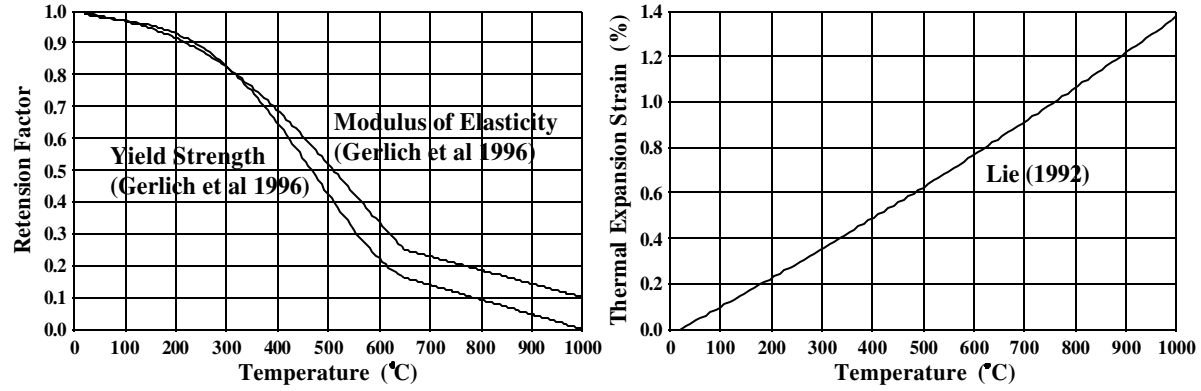


Figure 6. Cold Formed Steel Properties at Elevated Temperatures.

F_{yT} = steel yield strength at temperature T (in $^{\circ}\text{C}$),

E_T = modulus of elasticity of steel at temperature T (in $^{\circ}\text{C}$),

$E = 203000 \text{ MPa}$ = steel modulus of elasticity at room temperature, and

e_T = thermal elongation of steel at temperature T (in $^{\circ}\text{C}$) when heated from 20°C

At any time step during fire test simulation, the total deflection $y(x)$ of the steel joist, at any distance x from the left support, was computed as

$$y(x) = y_B(x) + y_D(x) \quad [4]$$

where $y_B(x) = 0.5 x (L - x) (e_T(T_H) - e_T(T_C)) / D \quad [5]$

$$y_D(x) = y_S(x) - y_0(x) \quad [6]$$

$$y_S(x) = \int_0^x \int_0^x f_S(x) dx \quad [7]$$

$$y_0(x) = ? x (L^3 - 2Lx^2 + x^3) / (24EI) \quad [8]$$

$y_B(x)$ = deflection due to stress-free thermal bowing (based on the assumption of linear thermal strain gradient across the joist section),

$y_D(x)$ = deflection due to deterioration of stiffness of the heated joist section,

$y_S(x)$ = deflection of heated joist due to tributary load ?,

$y_0(x)$ = initial deflection of unheated joist due to tributary load ?,

$L = 3805 \text{ mm}$ = joist span,

$e_T(T_H)$ = thermal strain of joist hot flange at temperature T_H , calculated using Equation 3,

$e_T(T_C)$ = thermal strain of joist cold flange at temperature T_H , calculated using Equation 3,

$D = 203.2 \text{ mm}$ = depth of the joist section,

$f_S(x)$ = curvature of heated joist section due to bending moment $M(x) = 0.5 ? x (L - x)$, caused by tributary load ?, and

I = moment of inertia of unreduced joist section about neutral axis perpendicular to the web.

JOIST program computes $y_S(x)$ values by dividing the joist span into 200 segments, calculating average curvature values $f_S(x)$ for each segment, and performing the double integration of Equation 7 numerically. The curvature values $f_S(x)$, for corresponding moments $M(x)$, are found from moment-curvature relationships that are generated at each time step (i.e. for every T_H and T_C temperature input pair). The program computes the

Table 6. Comparison of Predicted Failure Times with Test Results.

Assembly number	Structural failure time in test (min.)	JOIST predictions based on measured temperatures (min.)	JOIST predictions based on simulated temperatures (min.)
FF-22	73	73	71
FF-23	67	65	63
FF-24	68	66	63
FF-25	46	45	43
FF-27	61	56	55

non-linear moment-curvature relationships using the standard iterative procedures of sectional analysis based on the assumption of linear variation of mechanical (stress-related) strains across the joist section (i.e. the common ‘plain sections remain plain’ assumption) and the equilibrium of tensile and compressive forces. For these iterations, the effective joist section is divided into 100 two-dimensional elements with assigned temperatures (and associated mechanical properties of Equations 1 and 2) based on the distance of the element from the hot flange (linear temperature gradient assumed). The width of top flanges (under compressive stress) is reduced in effective cross-sections in accordance with Clause 5.6.2. of S136-94⁹ to account for local buckling effects. It is assumed that effective cross-section dimensions are insensitive to temperature, thus, they are computed based on steel properties at room temperature and compressive stress $f = F_y$.

Simulated mid-span deflection histories are presented in Figure 5 (lines with symbols). For these simulations, average temperatures measured at generalized locations 2a and 4a (Figure 1) were used for T_H and T_C input. Calculated deflections are in reasonable agreement with measured deflections; however, it should be mentioned that simulated deflection history for test FF-25, shown in Figure 5, was calculated using a reduction coefficient of 0.8 for $y_B(x)$ values. Initial JOIST simulations of this test significantly overestimated measured deflections. It could be presumed, that the presence of rock fibre insulation in Test FF-25 delays temperature rise in joist webs causing significant non-linearity in temperature (and thermal strain) gradients across joist sections. Such non-linearity leads to reduced thermal bowing and associated state of internal stress that has an unloading effect. In general, inspection of detailed numerical output (and hand calculation checks) indicated that thermal bowing deflections $y_B(x)$ in all tests constitute more than 85% of the total deflection $y(x)$ at any time except for the last one-two minutes before structural failure. Deflection component $y_D(x)$, associated with the deterioration of joist stiffness due to heating, does not contribute much to floor deflections until the initiation of the failure mechanism (i.e. until the reduced bending capacity of heated joist approaches the level of the bending moment acting at joist mid-span).

The JOIST program is designed to generate predictions of structural failure times by conducting failure checks at every time step of the simulation using the following criterion:

$$M_R < M(0.5L)$$

where

$M(0.5L) = 0.125 \cdot L^2 =$ bending moment at joist mid-span due to tributary load \cdot , and

M_R = inelastic bending capacity of effective cross-section of heated joist, where tensile strains (in the hot flange) are not limited, but compressive strains (in the cold flange) are limited to yield strain. This formulation of M_R is consistent with Clause 6.4.2. of S136-94⁹, and the program performs the necessary calculations using iterative sectional analysis procedures described above.

Table 6 lists JOIST predictions of structural failure times, for considered LSF floor tests, based on measured and TRACE-simulated temperatures. As expected, predictions based on measured temperatures show somewhat better agreement with test results than predictions based on simulated temperatures. All predictions are slightly below test results, and that is consistent with somewhat conservative failure criterion and assumptions used in the model.

CONCLUSION

A comprehensive thermal-structural model was presented for the assessment of fire resistance of unrestrained LSF floors. Numerical techniques were demonstrated in retrospective simulations of five standard tests. Characteristic patterns in thermal transmission and structural behaviour were discussed. The presented model is relatively simple in use, and it takes account of all significant parameters. Simulated temperature and deformation histories showed a reasonable agreement with experimental data. The structural failure criterion, used in the model, resulted in conservative and fairly accurate predictions of fire resistance.

REFERENCES

- ¹ Canadian Commission on Building and Fire Codes, National Building Code of Canada, National Research Council of Canada, Ottawa, Ontario, Canada, 1995.
- ² CAN/ULC-S101-M89, Standard Methods of Fire Endurance Tests of Building Construction and Materials, Underwriters' Laboratories of Canada, Scarborough, Ontario, Canada, October 1989.
- ³ ASTM E119-95a, Standard Test Methods for Fire Tests of Building Construction and Materials, American Society for Testing and Materials, West Conshohocken, PA, June 1995.
- ⁴ Alfawakhiri, F., and Sultan, M.A., Fire Resistance of Loadbearing LSF Assemblies, Proceedings of the Fifteenth International Specialty Conference on Cold Formed Steel Structures, St. Louis, Missouri, October 19-20, University of Missouri-Rolla, MO, 2000, pp. 545-561.
- ⁵ Alfawakhiri, F., and Sultan, M.A., Numerical Modelling of Steel Members Subjected to Severe Thermal Loads, Proceedings of the Seventh International Conference on Fire and Materials, San Francisco, CA, January 22-24, Interscience Communications Limited, UK, 2001, pp. 483-494.
- ⁶ Sultan, M. A., Seguin, Y. P., and Leroux, P., Results of Fire Resistance Tests on Full-Scale Floor Assemblies, Internal Report No. 764, Institute for Research in Construction, National Research Council of Canada, Ottawa, Ontario, Canada, May 1998.
- ⁷ CAN/CSA-A82.27-M91, Gypsum Board, Canadian Standards Association, Etobicoke, Ontario, Canada, 1991.
- ⁸ ASTM C36-97, Standard Specification for Gypsum Wallboard, American Society for Testing and Materials, West Conshohocken, PA, June 1997.
- ⁹ S136-94, Cold Formed Steel Structural Members, Canadian Standards Association, Etobicoke, Ontario, Canada, 1994.
- ¹⁰ Gerlich J.T., Collier P.C.R. and Buchanan A.H., Design of Light Steel-Framed Walls for Fire Resistance, Fire and Materials, Vol. 20, No. 2, 1996, pp. 79-96.
- ¹¹ Lie T.T. (Ed.), Structural Fire Protection, American Society of Civil Engineers, New York, NY, 1992.